polyaniline have been determined: phenyl-capped tetramer salt doped with 2 BF_4^- and one acetonitrile per tetramer in the cell, 1.39 g/cm^3; phenyl-capped dimer, 1.25 g/cm^3 [R. H. Baughman, J. F. Wolf, H. Eckhardt, L. W. Shacklette, *Synth. Met.* **25**, 121 (1988)].
24. Z. H. Wang, E. M. Scherr, A. G. MacDiarmid, A. J. Epstein, *Phys. Rev. B* **45**, 4190 (1992).
25. H. H. S. Javadi, K. R. Cromack, A. G. MacDiarmid, A. J. Epstein, *ibid.* **39**, 3579 (1989).
26. D. C. Dube, M. T. Lanagan, J. H. Kim, S. J. Jang, *J. Appl. Phys.* **63**, 2466 (1988).
27. Evacuated at 25°C and 10^{-5} torr for 12 hours.
28. L. Zuppiroli, F. Beuneu, J. Mory, P. Enzel, T. Bein, *Synth. Met.* **55–57**, 5081 (1993).
29. We are grateful for partial funding from the Sprague Electric Company. The contribution of S. Esnouf to the ac conductivity measurements is greatly appreciated.

16 February 1994; accepted 22 April 1994

Role of Deep Cloud Convection in the Ozone Budget of the Troposphere

Jos Lelieveld and Paul J. Crutzen

Convective updrafts in thunderstorms prolong the lifetime of ozone (O_3) and its anthropogenic precursor NO_x [nitric oxide (NO) + nitrogen dioxide (NO_2)] by carrying these gases rapidly upward from the boundary layer into a regime where the O_3 production efficiency is higher, chemical destruction is slower, and surface deposition is absent. On the other hand, the upper troposphere is relatively rich in O_3 and NO_x from natural sources such as downward transport from the stratosphere and lightning; convective overturning conveys the O_3 and NO_x toward the Earth's surface where these components are more efficiently removed from the atmosphere. Simulations with a three-dimensional global model suggest that the net result of these counteractive processes is a 20 percent overall reduction in total tropospheric O_3. However, the net atmospheric oxidation efficiency is enhanced by 10 to 20 percent.

Deep cumulonimbus (Cb) convection is a primary mechanism for transporting heat, moisture, and momentum from the lower to the upper troposphere, thus forcing the general circulation of the atmosphere (*1*). In the Cb outflow region in the cold upper troposphere, cirrus clouds develop and cover areas much larger than the cores of these convective systems. The vigorous motions in the Cb cores, which tend to maximize in the mid-troposphere, are driven by the release of latent heat by condensation (*2*). Conversely, mesoscale descent in the cloud environment is caused by radiative and evaporative cooling and melting of ice (*3*). Upward transport through Cb clouds takes about 0.5 to 1 hour, whereas the mesoscale subsidence takes about 10 to 50 hours over a proportionally larger area (*4*). Although thunderstorms constitute a major force in the convective overturning of the troposphere, especially in the tropics, synoptic disturbances such as extratropical cyclones also cause rapid vertical mixing; vertical velocities in these systems are highest in the region of organized convection ahead of the frontal zone (*5*). Deep convective motions play an important role in the vertical redistribution of trace gases (*6*). In their absence, surface-emitted pollutants would be transported to the upper troposphere in several months, whereas through their presence large parts of the troposphere are mixed on much shorter time scales. In this study, a global three-dimensional transport–chemistry model of the troposphere was used to evaluate the effects of convection on the chemistry and distribution of O_3.

Ultraviolet radiation causes the photochemical formation of O_3; in the background troposphere this occurs mostly through the oxidation of carbon monoxide (CO) and methane (CH_4), catalyzed by NO_x (*7*). The global budgets of these gases are dominated by anthropogenic emissions in the lower troposphere, notably from combustion (Table 1). In addition, in polluted or forested areas the oxidation of reactive hydrocarbons can play a significant role. In this study, we are concerned with the background troposphere; thus, we concentrate on the effects of CO and CH_4 oxidation. The lifetime of NO_x in the troposphere is about 1 to 2 days, and that of CO is a few months. Hence, convection strongly alters the vertical profiles of these species, particularly that of NO_x. The photochemical O_3 yield per emitted NO_x molecule decreases as NO_x concentrations increase (*8*), so that the convective dilution of surface-emitted NO_x from the boundary layer into the free troposphere enhances the formation of O_3. Moreover, the lifetime of NO_x in the upper troposphere is longer by up to an order of magnitude than in the boundary layer. Chemical conversions and dry deposition act on NO_2 rather than NO. Ultraviolet radiation fluxes and thus photolysis rates are relatively high and temperatures are low in the upper troposphere, which shifts the equilibrium between NO_2 and NO toward NO. Also, in the absence of deposition processes nitric acid (HNO_3) accumulates so that NO_x can partly reform through photodissociation and reaction with hydroxyl (OH). Furthermore, the lifetime of O_3 that has been formed photochemically in the boundary layer is enhanced by upward convective transport. At low altitudes, O_3 is efficiently destroyed by deposition on land surfaces (*9*) and through O_3 photolysis and subsequent reaction of $O(^1D)$ with water vapor; the latter reaction, yielding OH, is most efficient in the humid lower troposphere. Consequently, it has been concluded that convective transport of O_3 and its surface-emitted precursors enhances the tropospheric O_3 abundance (*6*, *10*). We show, however, that this assessment may not be true.

In the classical theory regarding tropospheric O_3, downward transport from the stratosphere is the dominant O_3 source (*11*). Although there is no agreement about the relative contributions of downward O_3 mixing and in situ photochemical O_3 formation, several studies suggest that the anthropogenic release of O_3 precursors is of major importance in the contemporary tro-

Table 1. Model trace-gas emissions (in teragrams per year) (*16*), of which two-thirds are from anthropogenic sources in the lower troposphere.

Source	CO	CH_4	NO_x
Fossil fuel use	450	115*	25
Biomass burning	400	30	9
Natural	470†	135‡	11.5§
NMHC oxidation	230‖		
Ruminants		105¶	
Rice paddies		70	
Landfills		40	
Sewage		25	
Total	1550	520	45.5

*Includes 5 Tg/year from CH_4 hydrate destabilization. †Three hundred teragrams per year from natural nonmethane hydrocarbon (NMHC) oxidation in the atmosphere, 100 Tg/year from vegetations, 40 Tg/year from oceans, and 30 Tg/year from wildfires. ‡Thirty teragrams per year from high-latitude wetlands and 70 Tg/year from low-latitude wetlands, 20 Tg/year from termites, 10 Tg/year from oceans, and 5 Tg/year from wild ruminants. §Five teragrams of N per year from lightning, 6 Tg of N per year from soils, 0.5 Tg from the stratosphere. ‖From anthropogenic NMHC oxidation in the atmosphere. ¶Includes 25 Tg/year from animal wastes.

J. Lelieveld, Wageningen University, Air Quality Department, Post Office, Box 8129, 6700 EV Wageningen, Netherlands.
P. J. Crutzen, Max-Planck-Institute for Chemistry, Atmospheric Chemistry Division, Post Office Box 3060, 55020 Mainz, Germany and the Center for Clouds, Chemistry, and Climate, University of California, San Diego, CA 93093-0221, USA.

posphere, particularly in the Northern Hemisphere (*7, 12*). Much of this O_3 is formed in the lower troposphere where the anthropogenic NO_x perturbation is strongest. The global release of NO_x from fossil fuel and biomass combustion is about 34 Tg/year (1 Tg = 10^{12} g), which is three-quarters of the estimated total source (Table 1). However, natural emissions from soils, lightning, and downward transport from the stratosphere are also significant, in particular in the background troposphere (*13*). Moreover, lightning and deep convection occur simultaneously so that much of the NO_x is deposited in the upper troposphere.

The global three-dimensional model that we used simulates the transport of chemical species based on monthly averages of observed winds (*14*). Its resolution is 10° by 10° horizontally and 100-hPa layers vertically up to the tropopause. Key components in the representation of the large-scale photochemistry of the troposphere are CH_4, CO, O_3, NO_x, and OH; the model accounts for processes in the gas, liquid, and aerosol phases, including removal of NO_x by aerosols and clouds (*15*). Emissions of CH_4 and CO were based on results of an earlier study (*16*), in which surface concentrations were prescribed on the basis of measurements, followed by calculations of CH_4 and CO losses by chemistry and transport from the source regions (Table 1). Emissions of NO_x from industrial sources and biomass burning were scaled to those of CO_2 (*15*). We assumed that NO_x production by lightning contributes 5 Tg/year. We reduced NO_x fluxes from soils compared to earlier model versions (*15*) to account for efficient local recycling of NO_2 in the vegetation canopy (*16*). We parameterized stratosphere-troposphere exchange of O_3 on the basis of large-scale seasonal air-mass fluxes and measured lower stratospheric O_3 concentrations (*17*). The resulting annual downward O_3 fluxes at northern and southern mid-latitudes are 405 and 186 Tg, respectively, whereas 63 Tg is transported to the stratosphere in the tropics (Table 2). We modeled deep convective air mass exchange as a stochastic process on the basis of the frequencies of Cb occurrence (*18*). The model accounts for entrainment and detrainment of air to and from the Cb clouds. Mass balance is achieved by subsidence in the mesoscale cloud environment. The model calculated upward convective mass fluxes, and the compensating downward motions are within the range of observations (*2, 18*).

The results from our model simulations (Table 2) corroborate studies suggesting that the global O_3 budget of the contemporary troposphere is strongly affected by photochemical formation from anthropogenically emitted trace gases (*7, 12, 15*). The calculated net O_3 flux from the stratosphere into the troposphere is 528 Tg/year, whereas net photochemical O_3 formation contributes 427 Tg/year (Table 2). It thus appears that these sources are comparable. However, the individual photochemical production and destruction terms approximately doubled because of anthropogenic emissions (*16*). The net difference is balanced by dry deposition, largely over land (Table 2). Two-thirds of the calculated global net O_3 production occurs in the mid-latitudes in the Northern Hemisphere, associated with industrial and traffic emissions (net 367 Tg/year at latitudes north of 30°N). We calculate that anthropogenic processes contribute 105 Tg (40%) to the annual mean O_3 column of 253 Tg in the contemporary global troposphere. Furthermore, we calculate that emissions from biomass burning in the tropics and subtropics also contribute strongly to O_3 formation; however, O_3 destruction is also enhanced, so that the net O_3 production from this source in the latitude belt between 30°S and 30°N is 108 Tg/year. The O_3 from biomass burning is supplemented by O_3 of stratospheric and industrial origin, which is transported southward from the northern mid-latitudes to the tropical regions. This transport occurs on a time scale of weeks to months, during which additional O_3 is formed but also the reactive O_3 precursors are removed. Subsequently, the remaining

Table 2. Calculated O_3 budget of the troposphere (in teragrams for column O_3 and teragrams per year for all other components). The hemispheres can be conceived as segregated O_3 reservoirs because interhemispheric O_3 exchange in the troposphere is small.

Component	90°S to 30°S	30°S to 0°	0° to 30°N	30°N to 90°N	Global
Column O_3 (Tg)	42	57	74	80	253*
Stratosphere → troposphere	186	−9	−54	405	528
O_3 formation†	262	1032	1243	1072	3609
O_3 loss‡	188	962	1327	705	3182
Net chemistry	74	70	−84	367	427
Dry deposition	135	186	261	371	953

*Two hundred fifty-three teragrams of O_3 ~25 Dobson units. †Mostly through the reactions HO_2 + NO and CH_3O_2 + NO. ‡Mostly through the reactions $O(^1D) + H_2O$, $O_3 + HO_2$, O_3 + OH, and $O_3 + O_2^-$ (the latter in clouds).

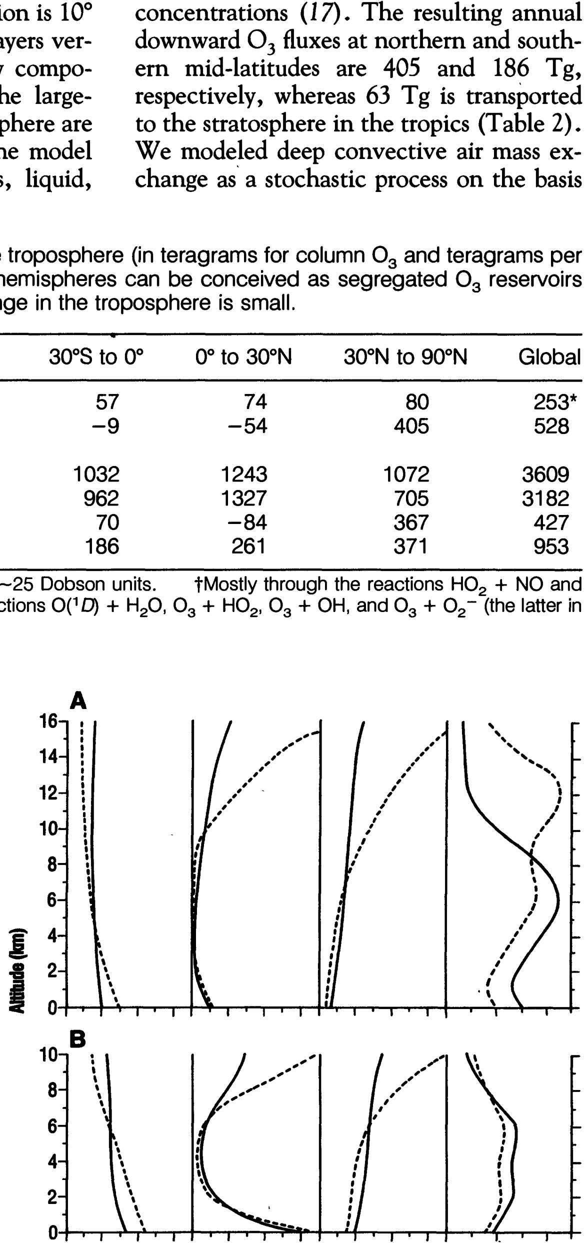

Fig. 1. Model-simulated zonal average vertical profiles of CO, NO_x, and O_3 volume mixing ratios and OH concentrations (**A**) in the tropics (5°N) and (**B**) in northern mid-latitudes (45°N) in July, including (solid lines) and excluding (dashed lines) the influence of deep convection; ppbv, parts per billion by volume; pptv, parts per trillion by volume.

Table 3. Global O_3 budgets of the troposphere (in teragrams for column O_3 and teragrams per year for all other components) calculated with and without the effects of convection on trace-gas distributions. The O_3 fluxes from the stratosphere are fixed.

Component	No convection	With convection	Change (%)
Column O_3 (Tg)	315	253	−20
Chemical formation	3171	3609	+14
Chemical loss	2598	3182	+22
Net chemistry	573	427	−25
Dry deposition	828	953	+15

O_3 is subject to photochemical destruction, so that on an annual basis the latitude belt between the equator and 30°N is not only a major photochemical O_3 source but an even more important O_3 sink (Table 2).

The role of deep cloud convection in the tropospheric O_3 budget is clearly demonstrated if we omit the convective vertical exchange of trace gases from our model. Figure 1 shows some examples of calculated zonal average changes in the CO, NO_x, O_3, and OH profiles by convection. The calculated NO_x and O_3 reductions in the upper troposphere are striking; mixing ratios of these gases in the upper troposphere are unrealistic if we neglect the influence of convection. In the simulation including the effects of convection, the troposphere contained 62 Tg less O_3 than the simulation that did not include these effects. This value is roughly equivalent to 6 Dobson units, about 20% of the O_3 column in the troposphere without convection (Table 3). One important cause is that convectively induced subsidence in the cloud environment carries O_3 of stratospheric origin downward from the upper troposphere into a regime in which the O_3 lifetime is shortest. This transport causes a decrease of O_3 in the upper troposphere, which is only partly compensated by an increase in the lower atmosphere (Fig. 1). An additional influence on O_3 concentrations resulted from a decrease of the global tropospheric NO_x column from 0.25 Tg of N without convection to 0.17 Tg of N with convection, caused by the downward transport of relatively NO_x-rich air from the upper troposphere. There is some observational evidence that this convective NO_x reduction occurs and that it can cause a decrease of O_3 production. From vertical profiles, calculated on the basis of measurements over northern Australia by the National Aeronautics and Space Administration ER2 aircraft during the summer of 1987, it was concluded that convective mixing had suppressed formation of O_3 in the cloud-perturbed area (*19*). It may be expected that these convective NO_x and O_3 reductions are most pronounced in remote marine regions where surface sources of O_3 precursors are absent. Furthermore, oxidation reactions that lead to O_3 formation, for example, in polluted air parcels that are carried upward, become less efficient at lower temperatures and pressures. These negative effects compete with the enhanced formation of O_3 by vertical mixing of NO_x from the boundary layer throughout the troposphere. In the global budget this process increases the photochemical formation of O_3 by 14%, despite the 30% decrease of the NO_x column (Table 3). Thus, convection enhances the O_3 forcing by anthropogenic precursor emissions. On a larger scale, however, chemical O_3 destruction is intensified even more strongly so that net O_3 production declined by 25% (Table 3).

In spite of the 20% overall O_3 loss in the troposphere, the net effect of convection on the atmospheric oxidation efficiency is positive. The higher O_3 concentrations near the surface enhance OH production, mainly through O_3 photodissociation and the subsequent reaction with water vapor: $O(^1D) + H_2O \rightarrow 2OH$ (Fig. 1). This increase of OH weighs heavily in the oxidation efficiency as a result of higher number concentrations (higher pressures) and larger reaction rate coefficients (higher temperatures) in the lower part of the troposphere. Including convection increases CH_4 destruction by about 20% and destruction of CO by about 10%; the latter is less as a result of the convective redistribution of CO, which is insignificant for CH_4. Thus, although O_3 in the upper troposphere dominates its climate effects (*20*), O_3 in the lower troposphere to a large extent controls the atmospheric oxidation efficiency.

REFERENCES AND NOTES

1. H. Riehl and J. S. Malkus, *Geophysics* **6**, 503 (1958); E. N. Lorenz, *The Nature and Theory of the General Circulation of the Atmosphere* (World Meteorological Organization, Geneva, 1967); R. E. Newell *et al.*, *The General Circulation of the Tropical Atmosphere and Interactions with Extratropical Latitudes* (MIT Press, Cambridge, MA, 1974).
2. R. A. Houze and A. K. Betts, *Rev. Geophys.* **19**, 541 (1981).
3. W. R. Cotton and R. A. Anthes, *Storm and Cloud Dynamics* (Academic Press, San Diego, 1989).
4. S. A. Rutledge *et al.*, *Mon. Weather Rev.* **116**, 1409 (1988); R. H. Johnson, *ibid.* **12**, 1590 (1984).
5. B. W. Atkinson, *Meso-scale Atmospheric Circulations* (Academic Press, New York, 1981); R. A. Houze and P. V. Hobbs, *Adv. Geophys.* **24**, 255 (1982).
6. L. T. Gidel, *J. Geophys. Res.* **88**, 6587 (1983); R. B. Chatfield and P. J. Crutzen, *ibid.* **89**, 7111 (1984); R. J. Ferek, R. B. Chatfield, M. O. Andreae, *Nature* **320**, 514 (1987); R. R. Dickerson *et al.*, *Science* **235**, 460 (1987); M. Garstang *et al.*, *J. Geophys. Res.* **93**, 1528 (1988); K. E. Pickering *et al.*, *ibid.* **94**, 14875 (1989); J. R. Scala *et al.*, *ibid.* **95**, 17015 (1990); D. H. Ehhalt, F. Rohrer, A. Wahner, *ibid.* **97**, 3725 (1992); K. E. Pickering *et al.*, *ibid.* **95**, 14049 (1990).
7. P. J. Crutzen, *Pure Appl. Geophys.* **106–108**, 1385 (1973); J. Fishman and P. J. Crutzen, *Nature* **294**, 855 (1978).
8. The O_3 yield is defined as the number of O_3 molecules produced photochemically per precursor molecule; O_3 production is a nonlinear function of the NO_x concentration, which has an optimum at relatively low NO_x concentrations. S. C. Liu *et al.*, *J. Geophys. Res.* **92**, 4191 (1987); X. Lin, M. Trainer, S. C. Liu, *ibid.* **93**, 15879 (1988).
9. I. E. Galbally and C. R. Roy, *Q. J. R. Meteorol. Soc.* **106**, 599 (1980).
10. R. A. Brost *et al.*, *Tellus* **40B**, 5 (1988); R. B. Chatfield and A. C. Delany, *J. Geophys. Res.* **95**, 18473 (1990); K. E. Pickering *et al.*, *ibid.* **96**, 3099 (1991); K. E. Pickering *et al.*, *ibid.* **97**, 17985 (1992); K. E. Pickering *et al.*, *J. Atmos. Chem.* **14**, 297 (1992); C. J. Walcek, W. R. Stockwell, J. S. Chang, *Atmos. Res.* **25**, 53 (1990); W. T. Luke *et al.*, *J. Geophys. Res.* **97**, 20647 (1992); W. F. Ryan *et al.*, *ibid.*, p. 17963.
11. C. E. Junge, *Atmospheric Chemistry and Radioactivity* (Academic Press, New York, 1963); H. U. Dütsch, *Adv. Geophys.* **15**, 219 (1971).
12. W. L. Chameides and C. G. Walker, *J. Geophys. Res.* **78**, 8751 (1973); J. Fishman, S. Solomon, P. J. Crutzen, *Tellus* **31**, 432 (1979); J. A. Logan *et al.*, *J. Geophys. Res.* **86**, 7210 (1981); J. Fishman, F. M. Vukovich, E. V. Browell, *J. Atmos. Chem.* **3**, 299 (1985); A. M. Hough and R. G. Derwent, *Nature* **344**, 645 (1990); P. J. Crutzen, in *Composition, Chemistry and Climate of the Atmosphere*, H. B. Singh, Ed. (Van Nostrand Reinhold, Altenburg, Germany, in press).
13. B. A. Ridley, M. A. Carroll, G. L. Gregory, *J. Geophys. Res.* **92**, 2025 (1987); J. W. Drummond, D. H. Ehhalt, A. Volz, *ibid.* **93**, 15831 (1988); Y. Kondo *et al.*, *ibid.* **98**, 20527 (1993).
14. The model transport has been tested in tracer transport studies with ^{85}Kr and chlorofluorocarbons CFC-11 and CFC-12, indicating that large-scale meteorological features are well reproduced. P. H. Zimmermann, in *Air Pollution Modelling and Its Application VI*, H. Van Dop, Ed. (Plenum, New York, 1988), pp. 593–608; P. H. Zimmermann *et al.*, *Atmos. Environ.* **23**, 25 (1989); A. H. Oort, *Global Atmospheric Statistics* [*Natl. Oceanic Atmos. Adm. Prof. Pap.* 14 (1983), p. 1].
15. The model-calculated large-scale OH field has been tested by the simulation of CH_3CCl_3 emissions and chemical destruction, for which agreement with measurements within ±15% was obtained. P. J. Crutzen and P. H. Zimmermann, *Tellus* **43AB**, 136 (1991); F. J. Dentener and P. J. Crutzen, *J. Geophys. Res.* **98**, 7149 (1993); F. J. Dentener, thesis, University of Utrecht (1993); J. Lelieveld and P. J. Crutzen, *Nature* **343**, 227 (1990).
16. J. Lelieveld, in preparation.
17. Stratosphere to troposphere transport of O_3 occurs mostly by mid-latitude synoptic disturbances, of which the small-scale features in the tropopause region that control O_3 exchange are not well quantified. The downward O_3 transport from the stratosphere and seasonal and interhemispheric variations calculated by our model, resulting from the multiplication of prescribed air-mass fluxes and O_3 concentrations in the lower stratosphere, are in general agreement with earlier experimental and theoretical studies. J. R. Holton, *J. Atmos. Sci.* **47**, 392 (1990); W. D. Komhyr *et al.*, in *Ozone in the Atmosphere*, R. D. Bojkov, Ed. (Deepak, Hampton, VA, 1989), pp. 147–150; G. Vaughan, in *Tropospheric Ozone*, I. S. A. Isaksen, Ed. (Reidel, Dordrecht, Netherlands, 1988), pp. 125–135.
18. Convective motions occur on a small scale that cannot be resolved by a global model, so that the effects of these processes are calculated off-line and prescribed to the model through parameterization. Our model convection scheme has been tested by the comparison of calculated with measured vertical profiles of the short-lived tracer ^{222}Rn (exhaled from soils; half-life, 3.8 days). The scheme has also been compared to other vertical transport parameterizations and to meteorological observations. The introduction of a convection scheme in our and other global chemistry models substantially improves vertical distributions of short-lived tracers. However, variations among both calculated and observed vertical mass fluxes are large, and additional measurement data are needed. J. Feichter and P. J. Crutzen, *Tellus* **42B**, 100 (1990); R. A. Brost and M. Heimann, in *Air Pollution and Its Dispersion*, H. Van Dop, Ed. (Plenum, New York, 1991), pp. 465–483.
19. K. E. Pickering *et al.*, *J. Geophys. Res.* **98**, 8737 (1993).
20. A. A. Lacis, D. J. Wuebbles, J. A. Logan, *ibid.* **95**, 9971 (1990).
21. This work was performed as part of the Chemistry Program of the Center for Clouds, Chemistry, and Climate (C^4) at the University of California in San Diego, sponsored by the U.S. National Science Foundation.

1 February 1994; accepted 26 April 1994